Preparation and Properties of Waterborne Polyurethane/Antimony Doped Tin Oxide Nanocomposite Coatings via Sol–Gel Reactions

Haifeng Zhou,[1] Hua Wang,[1] Xingyou Tian,[1] Kang Zheng,[1] Qingtang Cheng[2]
[1]*Key Laboratory of Materials Physics, Institute of Solid State Physics, Chinese Academy of Sciences, Hefei 230031, China*

[2]*Jiangsu Hehai Nanometer Science and Technology Co., Ltd, Taixing 225401, China*

Various amounts of antimony doped tin oxide (ATO) nanoparticles were incorporated into waterborne polyurethane (WPU) dispersions by sol–gel reactions. The dispersion state and morphology investigated by transmission electron microscopy (TEM) and scanning electron microscopy (SEM) showed that the nanoparticles can disperse in the matrix uniformly. The analysis of visible–near infrared spectra (VIS–NIR) suggested that the WPU/ATO coatings show both low near infrared transmittance (35%) and high visible light transmittance (76%). The heat-insulation effect measurement demonstrated that the WPU/ATO coatings could prevent heat transmission effectively. It was also found that the introduction of ATO nanoparticles can improve the mechanical properties significantly. **POLYM. COMPOS., 35:1169–1175, 2014. © 2013 Society of Plastics Engineers**

INTRODUCTION

Polyurethanes (PUs) are one of the most versatile polymeric materials whose properties can be tailor-made by simply adjusting the compositions. Because of this, the PUs are of great interest for applications in foams, elastomers, adhesives, and coatings [1–9]. However, the conventional PU products usually contain a large number of organic solvents and sometimes even free isocyanate monomers which are harmful to the environment and human health. Therefore, they have been gradually replaced by WPU in the past decades because of increasing need to reduce volatile organic compounds (VOCs) and hazardous air pollutants (HAPs) [10–18]. Furthermore, compared with conventional organic solvent-borne PU, WPUs present several of the attractive advantages such as low viscosity at high molecular weight, nontoxicity, and good applicability.

Incorporation of inorganic nanoparticles into the polymers has been attracting increasing concerns recently. Much effort has been devoted to the investigation of hybrid inorganic/organic nanocomposite materials since inorganic nanoparticles not only can improve the properties of matrices but also can endow them with some new functions which are of great importance for their use in potential applications. ATO is a kind of important transparent conductive oxides exhibiting high optical transmission, infrared light insulation, electrical conduction, stability and low cost [19, 20]. It has been using in transparent electrodes, heat mirrors, displays, electro chromic windows, catalysts, rechargeable Li batteries, and transparent heat-insulating coatings [21–25]. For example, Xu et al. [25] prepared the antimony doped tin oxide (ATO)/waterborne polyurethane (WPU) nanocomposite via blending the WPU emulsion and ATO solution, and the nanocomposite presented good heat-insulating properties. However, the commercial ATO solution had been modified with surfactant before the mixing of WPU emulsion and ATO solution. In other words, the nanocomposite preparation consisted of two processes, one was the synthesis of WPU emulsion and the other was the modification of ATO. The modification ATO needed to add a large amount of organic solvent and surfactant which not only increased the preparation cost and time but also caused environmental issue. To prepare WPU/ATO nanocomposite coatings by one simple step, we had incorporated 3-aminopropyltriethoxysilane (APS) via the reaction of amino group of APS with the isocyanate group of polyurethane prepolymer chain. It is well known that the reactivity of amine groups towards the isocyanate is much high. Thus, the reaction between the isocyanate groups and the amine groups of APS is easy. The introduction of the alkoxysilane into polymer chain,

Correspondence to: Xingyou Tian; e-mail: xytian@issp.ac.cn
Contract grant sponsor: National Natural Science Foundation of China; contract grant number: 51103160.
DOI 10.1002/pc.22764
Published online in Wiley Online Library (wileyonlinelibrary.com).

this method, namely the sol–gel reaction, is an effective approach to produce hybrid inorganic/organic nanocomposites. As a very important alkoxysilane, 3-aminopropyltriethoxysilane (APS) has been wildly applicated in the modification of nanoparticles since the alkoxy can chemically bonded on the surfaces of the nanoparticles by condensation with surface hydroxyl groups of the nanoparticles. Compared with the method of physical blending, the sol–gel reaction not only can offer a simple way to prepare inorganic/organic nanocomposite by one simple step but also inhibit agglomerate of nanoparticles and offer strong interactions between the polymer and inorganic nanoparticles.

In this study, we prepared WPU/ATO nanocomposite coatings through sol–gel process by introducing the 3-aminopropyltriethoxysilane (APS) into the polyurethane prepolymer chain. The sol–gel process consists of the hydrolysis of the terminal alkoxyl groups under basic catalysis in the presence of water and subsequent condensation reactions of silanols with neighboring OH-groups on the particle surface. The obtained nanocomposites were characterized by SEM, transmission electron microscopy (TEM), mechanical properties, VIS–NIR spectra and heat-insulation effect measurements. And the result showed that preparing WPU/ATO nanocomposite coatings through sol–gel process is a simple and efficient method of synthesis WPU/ATO nanocomposite coatings.

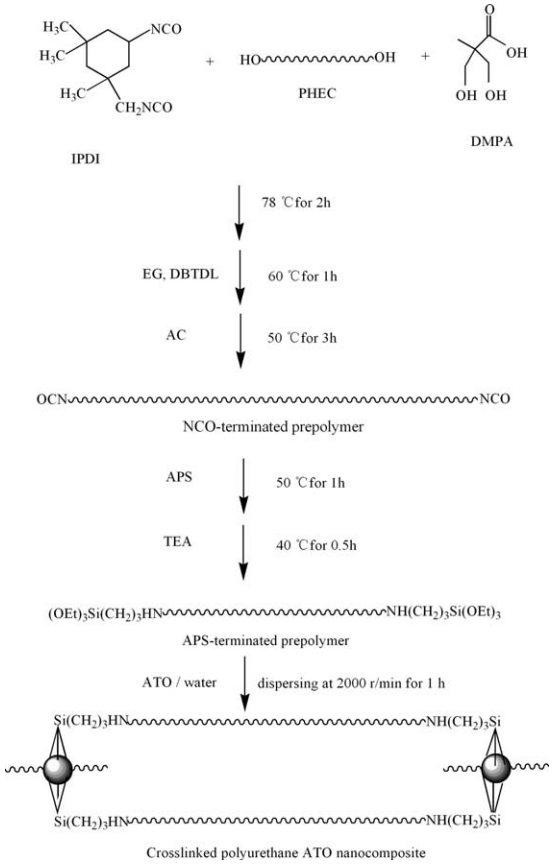

SCH. 1. An overall reaction scheme for preparing the WPU/ATO nanocomposites. The zig–zag-lines are used as general symbol for the polymer chains formed in the different steps.

EXPERIMENTAL

Materials

Isophorone diisocyanate (IPDI), dimethylolpropionic acid (DMPA), poly(1,6-hexyl 1,2-ethyl carbonate) diol (PHEC) ($M_w = 2{,}000$), were supplied by An Li Artificial Leather, Hefei, China. Dibutylamine, dibutyltin dilaurate (DBTDL), and ethylene diglycol (EG) were purchased from Su Yi Chemical Reagent, Shanghai, China. Acetone (Ac), 3-aminopropyltriethoxysilane (APS) were purchased from Qiang Shen Chemical Reagent, Nanjing, China. Antimony doped tin oxide (ATO) was purchased from Hu Zheng Nano Technology, Shanghai, China. The doping level of the antimony is 10 wt%. The raw materials were used as received, except for the polyols. The PHEC were dried in vacuo at 120°C for 2 h.

Preparation of WPU/ATO Dispersions

The overall reaction process for the synthesis of the composite is shown in Scheme 1. The PHEC (54 g), IPDI (30 g), and DMPA (3.3 g) were added to a four-necked flask equipped with a mechanical stirrer, nitrogen inlet, condenser, and thermometer. The reaction mixture was stirred and carried out at 78°C for 2 h under a dry nitrogen atmosphere. Upon reaching the theoretical NCO value (7.7 wt% NCO) which was determined by a dibutylamine back titration method, EG (5.5 g) and DBTDL were added. Stirring was continued for 1 h at 60°C and then AC was added to reduce the viscosity of the system. After an additional 3 h of reaction, APS (13.9 g) was added and allowed to react with the remaining free isocyanate groups at 50°C for 1 h, and then the reactants were cooled to room temperature and neutralized by the addition of TEA (2.5 g) for 30 min to neutralize all the carboxylic acid groups at 40°C. Meanwhile, the ATO was added to 200 ml water and sonicated for 30 min at room temperature. Then, the above mentioned ATO dispersion was added to the polyurethane to accomplish the dispersing at 2,000 r min^{-1} for 1 h with dispersing machine and the pH value was tuned to 8 with ammonia solution. Finally, Ac was removed using distillation equipment. The solid content of the resulting dispersion was adjusted to 30 wt%. By changing the contents of ATO over the range of 0, 1, 3, 5, and 10 wt%, a series of WPU/ATO dispersions were prepared and coded as WPU0, WPU1, WPU3, WPU5, and WPU10, respectively. The dispersions were poured into Teflon molds to dry at ambient temperature for 7 days to obtain films.

Characterization

Fourier transform infrared (FTIR) spectroscopy was performed on a spectrometer (Nexus, Nicolet) in the

 DOI 10.1002/pc

transmission mode in the range 400–4000 cm^{-1} at room temperature. Data were collected at 4 cm^{-1} resolution coadding 32 scans per spectrum. KBr disks were prepared after mixing (0.5%) each of the test samples with dry KBr. Wide angle X-ray diffraction measurement was carried out with a Philips X'pert-PRO using Cu Kα radiation. The diffraction angle 2θ ranged from 10° to 90°. The tensile properties of the films were measured at 25°C with a universal testing machine (CMT, SANS) at a crosshead speed of 300 mm min^{-1}. The reported values are averages obtained from five specimens. Morphology of the nanocomposite films was observed with a scanning electron microscope (FESEM, Sirion 200 FEI) at 10 KV. The specimens were frozen in liquid nitrogen, fractured, and then coated with gold. The morphology of the particles in the dispersion was obtained with a transmission electron microscope (JEM-2010). The dispersions were diluted to 0.5 wt%, and then 1 ml of the dispersion was deposited onto a carbon film grid. After drying, the samples were characterized. The WPU/ATO coatings were coated on glass and the final thickness of the films was about 100 μm. The transmittance of the glass with the WPU/ATO coatings was measured by UV3600 (Shimadzu, Japan) UV–VIS–NIR spectrophotometer. The transition mode was used and the wavenumber range was set from 400 to 2500 nm. The heat insulation effect measurement was tested in a self made polystyrene foam box covered with glass plates. One of the glass plates was coated with WPU/ATO. The heat-insulating effect of WPU/ATO coatings was characterized by measuring the changes of temperature every 10 min.

RESULTS AND DISCUSSION

Confirmation of Sol–Gel Reaction

To confirm the reaction between the APS and the OH groups on the surface of the ATO particles, model reactions were used to prepare the sample. The representative

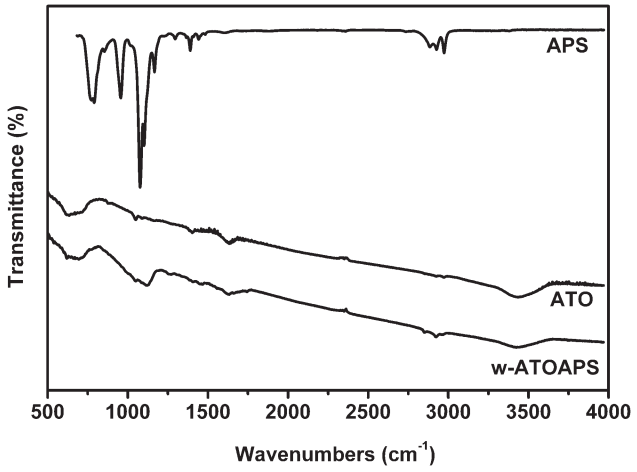

FIG. 1. FTIR of ATO before and after reaction with APS.

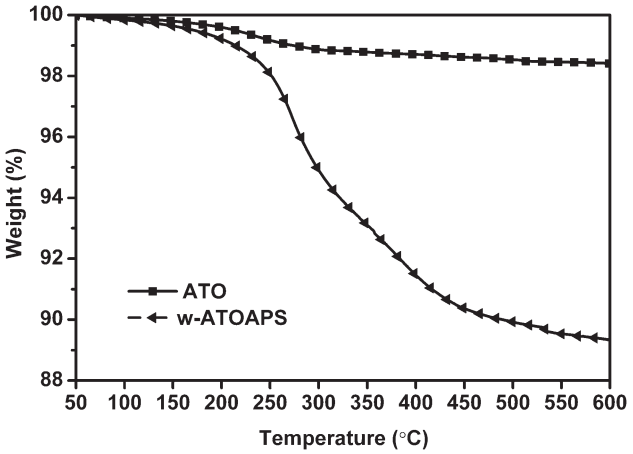

FIG. 2. TGA of ATO before and after reaction with APS.

samples used the same concentrations of water, APS, ammonia solution and ATO as for the preparation of the WPU, but in the absence of the other compounds. The reaction mixture was washed with ethanol and water three times. This sample was referred as "washed" w-ATOAPS. FTIR spectra of the virgin ATO and the modified ATO were shown in Fig. 1. It can be seen that the absorption bands of ATO are well separated from those of APS with a strong absorption band around 600 cm^{-1}, which is the characteristic absorption of ATO. The band at 1,060 and 1,401 cm^{-1} in the ATO sample is considered as an impurity. In addition, two strong absorption bands at 3431 and 1628 cm^{-1} were, respectively assigned to the stretching and bending vibration modes of water most likely adsorbed on the surface of ATO nanoparticles through H-bonding to OH groups. In the case of w-ATOAPS, two new absorption peaks located at 1051 and 1125 cm^{-1} (as referred to Si—O—Si and Si—O—C modes) indicating that APS has been chemically bonded to the surface of ATO particles through condensation reaction [26, 27]. The TGA curves also confirmed the condensation reactions between silanol groups and the surface hydroxyl groups on the metal oxide particles as can be seen from the Fig. 2. The virgin ATO starts to lose weight upon heating above 100°C, which is due to the release of water and some small organic molecules contained in the samples. Apart from a slight weight loss of virgin ATO, significant mass loss is observed when modified, which presumably assigned to the decomposition of chemically bonded silane molecules.

Confirmation of APS Capping by FT-IR Spectroscopy

The FT-IR spectra of the NCO-terminated PU and APS capped PU are shown in Fig. 3. It can be seen that the characteristic absorption peak at about 2,270 cm^{-1} corresponding to the stretch vibration of the NCO group has completely disappeared upon capping with APS [28, 29]. This confirms that APS has been incorporated into the polyurethane prepolymer chain.

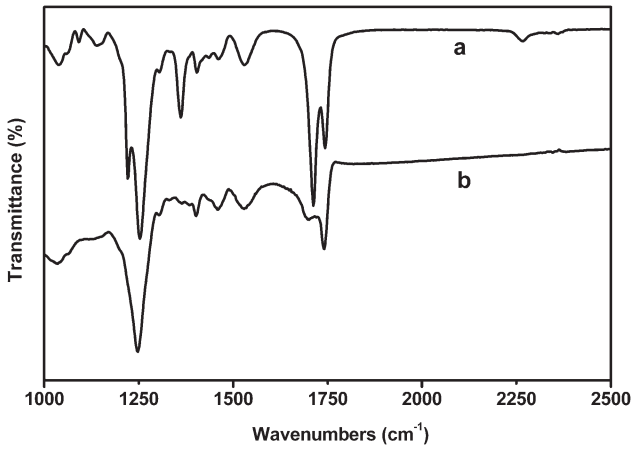

FIG. 3. FT-IR spectra of the PU prepolymer (a) before and (b) after APS capping.

Effect of APS Concentration on the Coatings

In preliminary experiments, we identified the optimal reaction conditions in terms of content of APS, PH value and time of high speed dispersion to get long time stable emulsion with different ATO loadings. To compare the effect of APS on the properties of WPU/ATO nanocomposite coatings, we synthesized the coatings without APS under the same conditions. It was found that the WPU/ATO dispersion without APS showed very poor stability (Fig. 4b) and it was difficult to obtain homogeneous film. The ATO nanoparticles tend to form large particles and sediment quickly due to the high surface energy. With the aim to determine the appropriate amount of APS, experiments with different APS loadings had been done. The nanocomposite coatings with a small amount of APS showed better stability than that without APS, however sediment presented at the bottom of the container gradually when the ATO loadings were high. While, the viscosity was very large when nanocomposite coatings with a large amount of APS since the crosslinking reaction happened during the dispersing step and more APS would lead to larger crosslinking density. Thus, we determined the optimal amount of APS (13 wt%) in our experiments which could limit the agglomerate of ATO nanoparticles effectively but without large viscosity of the coatings (Fig. 4a).

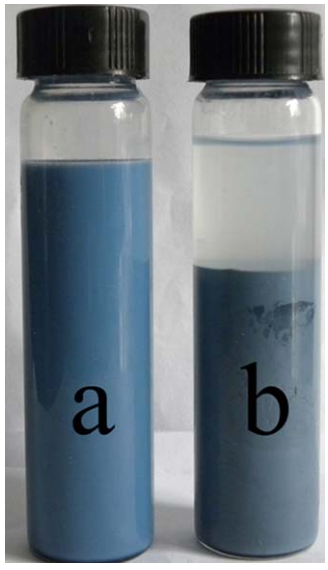

FIG. 4. Photograph of WPU10 coatings (a) with APS and (b) without APS. [Color figure can be viewed in the online issue, which is available at wileyonlinelibrary.com.]

XRD

Figure 5 shows the XRD patterns of the WPU/ATO nanocomposites with various ATO contents. ATO shows four well-defined diffraction peaks at 26.6°, 33.4°, 38.1°, and 51.8° of 2θ. For the neat WPU, there is only a broad diffraction hump at 20.5° of 2θ indicating the amorphous nature of the film [29]. It can be explained by the fact that polyurethane that has been prepared with amorphous PC usually shows no crystallinity. With an addition of ATO in the WPU matrix, some diffraction peaks appear in the diffractograms. As the ATO content in the films increases, the peaks become more pronounced. When it increases up to 3 wt%, four peaks at 26.6°, 33.4°, 38.1°, and 51.8° of 2θ are observed. Therefore, it can be inferred that these diffraction peaks in the nanocomposite materials are attributable to the ATO component. Furthermore it should be noted that no additional peak or peak shift in the diffraction angles is observed. Thus we can conclude that the diffractograms of nanocomposites are superimpositions of the diffractograms of the two components, and the ATO nanoparticles are embedded inside the polymer matrix uniformly and their presence does not change the amorphous nature of WPU and the crystal structure of themselves.

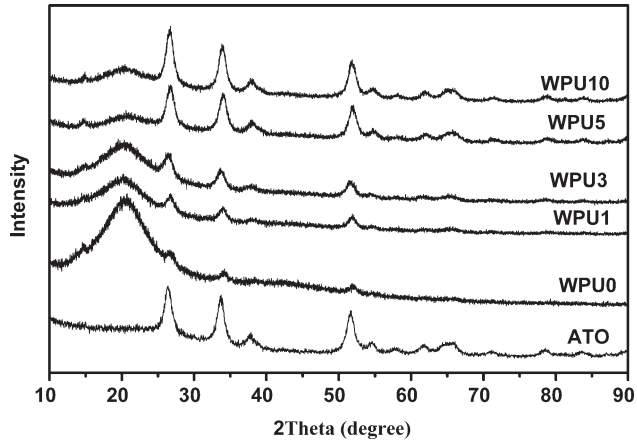

FIG. 5. XRD of ATO and WPU/ATO.

DOI 10.1002/pc

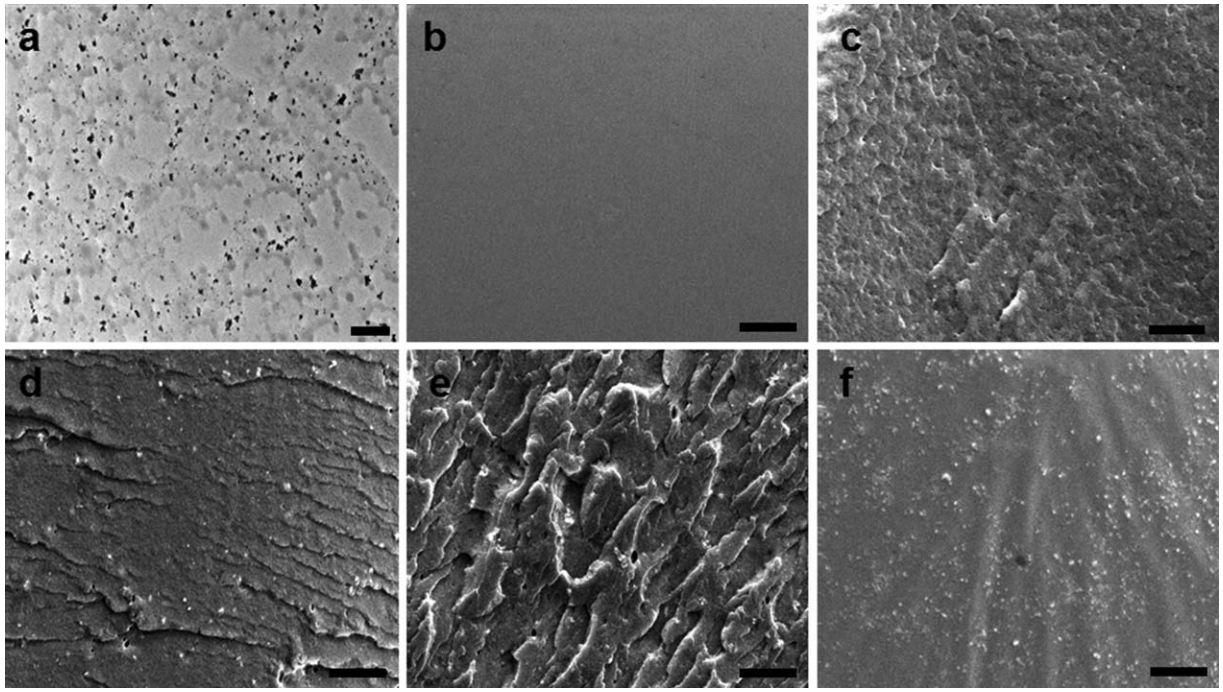

FIG. 6. TEM (a) of WPU10 dispersion (scale bar = 0.5 um), SEM (b–f) of WPU0,WPU1,WPU3, WPU5, WPU10 composites (scale bars = 20 μm).composites (scale bars= 20 μm).

TEM and SEM

To analyze the dispersion state and morphology of the WPU/ATO dispersions, TEM images were taken. Figure 6a shows the representative TEM image of the WPU dispersion filled with 10 wt% ATO. The light background represents the polyurethane phase while the dark dots represent the ATO nanoparticle phase. It can be seen that the ATO nanoparticles in PU film were well dispersed and the average diameter is <100 nm, though it has a slight aggregation. Furthermore, the morphology of ATO dispersed in the WPU matrix is also studied by scanning electron microscopy (SEM) images of the cross-sectional fractured surface of the composites. Figure 6b–f shows the images of neat WPU matrix and nanocomposites filled with 1, 3, 5, and 10 wt% ATO, respectively. Comparing with the WPU film, the distribution of the ATO can be easily identified. The ATO nanoparticles appear as white dots, whose concentration on the fracture surface of the nanocomposites is increased as the filler loading increasing. Obviously, no large aggregates and a homogeneous distribution of the ATO nanoparticles in the WPU matrix indicated that the interactions between fillers and matrix are strong and effective to overcome the van der Waals attraction existing between the ATO nanoparticles due to chemically bonded APS to the surface of ATO particles, thus the filler can disperse in the matrix uniformly [30]. Such even distribution of the fillers in the matrix plays an important role in the transparence and mechanical properties of the films.

Mechanical Properties

The mechanical behavior of the films with different content of ATO was investigated by tensile tests at room temperature. Typical tensile stress-strain behaviors are shown in Fig. 7. Two characteristic regions of deformation behavior can be observed. At low strains, the stress increases linearly with an increase of strain, and the Young's modulus was calculated from the initial slope in this elastic region. At higher strain, the deformation feature of the nanocomposite films greatly depends on the loading level of ATO. Table 1 summarizes the Young's modulus, tensile strength and elongation at break. The WPU0 showed a Young's modulus of 31.2 MPa, a tensile strength of 17 MPa, and an elongation at break of 260%. As the content of ATO increases, the Young's modulus and ultimate tensile strength increased, but its elongation at break decreased. The tensile strength increases significantly from 17 to 35 MPa with increasing filler content from 0 to 10 wt%, whereas the elongation at break decreased from 260 to 26%. Obviously, the ATO content has a profound effect on the tensile properties. This is attributed to the effects of ATO nanoparticles as cross-links which resulted in strong interactions between fillers and matrix and restricted the motion of the matrix. For the WPU/ATO nanocomposite containing 10 wt% ATO, Young's modulus is about 159 MPa, approximately five times higher than that the pure WPU film. This indicates that ATO nanoparticles augment rigidity and stiffness of the composites as reinforcing fillers.

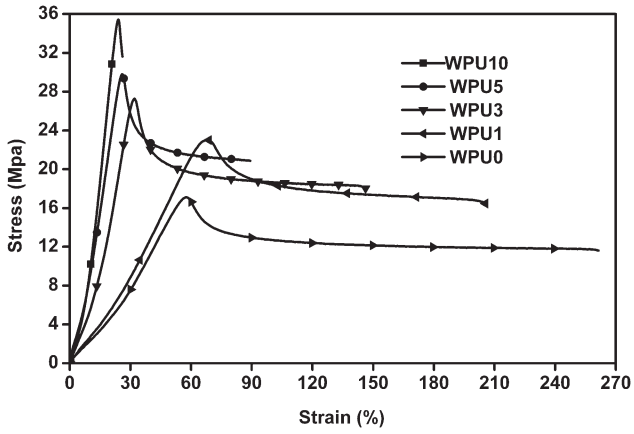

FIG. 7. Stress–strain curves of WPU/ATO films.

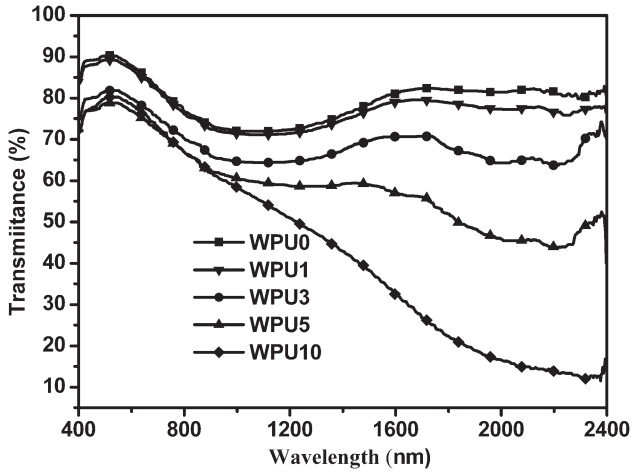

FIG. 8. VIS–NIR spectra of WPU/ATO coatings.

VIS–NIR Spectra and Heat Insulating Effect

It is generally believed that the introduction of inorganic fillers into a transparent matrix can give rise to the light scattering of an incident light ray because of different refractive index between the matrix and inorganic filler. The intensity of scattered light is dependent on the size of small regions generated from the aggregated inorganic fillers, which increases drastically when the size of the small region reaches the visible light wavelength [20]. The scattered light from the particles dispersed in the matrix lead to the decline of transparency of the coatings. To investigate how ATO content affects the optical transmission of the composite coatings, VIS–NIR spectra were performed. Figure 8 showed the transmittance for the composite coatings in the wavelength range of visible light (400–780 nm) and near infrared (780–2,400 nm) as a function of ATO content. And the transmittance of the above mentioned bands were calculated from the curves and was shown in Table 1. Compared with a pure WPU coating, the transmittance of WPU/ATO nanocomposite coatings in visible light begins to decline as ATO contents increasing and reduces to 76% when the ATO content was up to 10 wt%, which can attributed to the different refractive index that increase the light scattering of the WPU/ATO coatings. However, the loss of transmittance is not so remarkable indicating a fine and homogeneous random distribution of small aggregates, as evidenced by SEM analysis. Meanwhile, the change trend of near infrared transmittance is pronounced as can be seen in the Table 1, the pure WPU coatings has a 78% transmittance more than two times of that WPU/ATO with 10 wt% ATO content. Thus, it is anticipated that WPU/ATO coatings will provide good heat insulating effect. To investigate it, we test the heat insulating effect by a self-made heat-insulating box. Figure 9 showed the temperatures of WPU/ATO coatings along the irradiation time. It can be seen that the temperature of the room with ATO/PU coatings was always lower than that of pure WPU coatings. As to the WPU10 and WPU0 the temperature difference begins to increase as time going on and then leveled off to 29°C. This verified that the WPU/ATO coatings can prevent heat transmission and heat diffusion effectively.

TABLE 1. Mechanical properties and transmittance of the WPU/ATO coatings.

				Transmittance (%)	
Sample	E (MPa)[a]	σ (MPa)	ε (%)	Near infrared (780–2,400 nm)	Visible (400–780 nm)
WPU0	31.2	17	260	78	86
WPU1	36.5	23	205	76	84
WPU3	90.6	27	144	67	80
WPU5	124	29	88	55	78
WPU10	159	35	26	35	76

[a]Young's modulus, σ = tensile strength, ε = elongation at break.

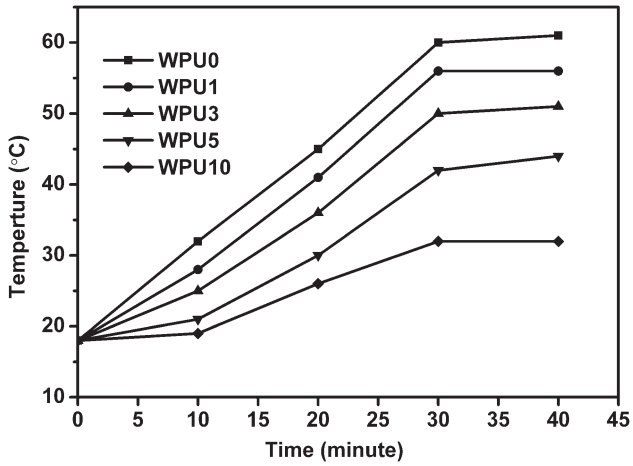

FIG. 9. Relationship between the temperature and irradiation time for WPU/ATO coatings. Relationship between the temperature and irradiation time for WPU/ATO coatings.

DOI 10.1002/pc

CONCLUSIONS

WPU/ATO nanocomposite coatings were prepared via sol–gel reactions. The mechanical properties of the nanocomposite improved as the ATO loadings increasing. WPU10 gives the tensile strength of 35 Mpa and Young's modulus of 159 MPa, corresponding to 200 and 510% enhancement as compared with pure WPU. The transmittance of WPU/ATO films in the band of visible light and near infrared as a function of ATO content were calculated from the VIS–NIR spectra. The results indicated that the WPU/ATO coatings had significant near infrared transmittance (35%) without pronounced loss of visible light transmittance (76%) when the ATO content up to 10 wt%. This result is directly related to the good dispersion of nanoparticles which were studied by TEM and SEM. Moreover, the heat-insulation effect measurement verified that the WPU/ATO coatings could prevent heat transmission effectively. Thus, together with visible light transmittance results, we can conclude that preparation of WPU/ATO nanocomposite coatings via sol–gel reactions allows the simple design and realization of high transparency and efficient heat insulation coatings.

REFERENCES

1. Z.S. Petrovic and J. Ferguson, *Prog. Polym. Sci*., **16**, 695 (1991).
2. Y.J. Li, K.H. Matthews, T.M. Chen, Y.F. Wang, M. Kodama, and T. Nakaya, *Chem. Mater*., **8**, 1441 (1996).
3. K.D. Weiss, *Prog. Polym. Sci*., **22**, 203 (1997).
4. M. Sobczak, C. Debek, E. Oledzka, G. Nalecz-Jawecki, W.L. Kolodziejski, and M. Rajkiewicz, *J. Polym. Sci. Polym. Chem*., **50**, 3904 (2012).
5. J. Vega-Baudrit, M. Sibaja-Ballestero, P. Vazquez, R. Torregrosa-Macia, and J.M. Martin-Martinez, *Int. J. Adhes. Adhes*., **27**, 469 (2007).
6. Y. Wang, G.A. Sotzing, and R.A. Weiss, *Chem. Mater*., **20**, 2574 (2008).
7. W.M. Huang, B. Yang, Y. Zhao, and Z. Ding, *J. Mater. Chem*., **20**, 3367 (2010).
8. N. Athanasopoulos, A. Baltopoulos, M. Matzakou, A. Vavouliotis, and V. Kostopoulos, *Polym. Compos*., **33**, 136 (2012).
9. V. Garcia-Pacios, V. Costa, M. Colera, and J.M. Martin-Martinez, *Prog. Org. Coat*., **71**, 1302 (2011).
10. B.K. Kim, *Colloid. Polym. Sci*., **274**, 599 (1996).
11. B.K. Kim, S.Y. Lee, J.S. Lee, S.H. Baek, Y.J. Choi, J.O. Lee, and M. Xu, *Polymer*, **39**, 2803 (1998).
12. J. Huybrechts, P. Bruylants, A. Vaes, and A. De Marre, *Prog. Org. Coat*., **38**, 67 (2000).
13. S.A. Madbouly, J.U. Otaigbe, A.K. Nanda, and D.A. Wicks, *Macromolecules*, **38**, 4014 (2005).
14. S.H. Hsu, H.J. Tseng, and Y.C. Lin, *Biomaterials*, **31**, 6796 (2010).
15. Q. Zhang, J. Hu, and S. Gong, *J. Appl. Polym. Sci*., **122**, 3064 (2011).
16. X. Wang, Y.A. Hu, L. Song, W.Y. Xing, H.D. Lu, P. Lv, and G.X. Jie, *Surf. Coat. Tech*., **205**, 1864 (2010).
17. F.X. Qiu, H.P. Xu, Y.Y. Wang, J.C. Xu, and D.Y. Yang, *J. Coat. Technol. Res*., **9**, 503 (2012).
18. A.K. Nanda and D.A. Wicks, *Polymer*, **47**, 1805 (2006).
19. Y. Wang, T. Brezesinski, M. Antonietti, and B. Smarsly, *Acs Nano*., **3**, 1373 (2009).
20. A. Wakabayashi, Y. Sasakawa, T. Dobashi, and T. Yamamoto, *Langmuir*, **23**, 7990 (2007).
21. Y.C. Wang and C. Anderson, *Macromolecules*, **32**, 6172 (1999).
22. A. Wakabayashi, Y. Sasakawa, T. Dobashi, and T. Yamamoto, *Langmuir*, **22**, 9260 (2006).
23. A.M. Volosin, S. Sharma, C. Traverse, N. Newman, and D.-K. Seo, *J. Mater. Chem*., **21**, 13232 (2011).
24. J. Feng, B. Huang, and M. Zhong, *J. Colloid. Interf. Sci*., **336**, 268 (2009).
25. Z. Dai, Z. Li, L. Li, and G. Xu, *Polym. Adv. Technol*., **22**, 1905 (2011).
26. N. Frickel, R. Messing, T. Gelbrich, and A.M. Schmidt, *Langmuir*, **26**, 2839 (2010).
27. C. Bressy, N. Van Giang, F. Ziarelli, and A. Margaillan, *Langmuir*, **28**, 3290 (2012).
28. D.H. Jung, H.M. Jeong, and B.K. Kim, *J. Mater. Chem*., **20**, 3485 (2010).
29. A. Kultys, M. Rogulska, S. Pikus, and K. Skrzypiec, *Eur. Polym. J*., **45**, 2629 (2009).
30. W. Posthumus, P. Magusin, J.C.M. Brokken-Zijp, A.H.A. Tinnemans, and R. van der Linde, *J. Colloid. Interf. Sci*., **269**, 109 (2004).